

Measurement of atomic diffraction phases induced by material gratings

John D. Perreault and Alexander D. Cronin
University of Arizona, Tucson, Arizona 85721
 (Dated: November 13, 2018)

Atom-surface interactions can significantly modify the intensity and phase of atom de Broglie waves diffracted by a silicon nitride grating. This affects the operation of a material grating as a coherent beam splitter. The phase shift induced by diffraction is measured by comparing the relative phases of several interfering paths in a Mach-Zehnder Na atom interferometer formed by three material gratings. The values of the diffraction phases are consistent with a simple model which includes a van der Waals atom-surface interaction between the Na atoms and the silicon nitride grating bars.

PACS numbers: 03.75.Be, 03.75.Dg, 39.20.+q, 34.20.Cf

Keywords: atom interferometry, atom optics, van der Waals, atom-surface interactions

A coherent beam splitter is a useful component for constructing an atom interferometer [1]. The purpose of the beam splitter is to generate a quantum superposition of atom waves, propagating along two paths which can be recombined to form an interference pattern. The contrast and phase of the interference pattern can then be used to study interactions that affect the atoms differently in the two interferometer paths. However, atom beam splitters formed using laser light [2, 3, 4] and material grating structures [5] can create beams with differing complex amplitudes. A familiar analogy of this in optics occurs for light beam splitters formed using glass plates, thin metal films, and multi-layer dielectric stacks which all cause a phase shift between the reflected and transmitted components [6]. These complex amplitudes are an important concern when building an atom interferometer since they affect the phase and contrast of the interference pattern, and have been identified as a source of uncertainty for atom interferometer gyroscopes [7]. Here we present the first evidence of beam splitter induced phase shifts in an atom interferometer based on material gratings and a new method for measuring these phase shifts for interferometers that utilize diffraction.

The van der Waals (vdw) atom-surface interaction [8] plays a significant role in determining the intensity and phase (diffraction phase) of atom waves split by a material grating. Several atom-optics experiments have observed how atom-surface interactions can affect the intensity of atom waves [5, 9, 10]. By comparison, few experiments have directly measured the diffraction phases induced by atom-surface interactions [11]. In this Letter the first and second order diffraction phases are measured by comparing the phase difference between the various interfering paths in a three grating Mach-Zehnder atom interferometer.

The experimental setup used to measure the atomic diffraction phases induced by a material grating is shown in Fig. 1. A Mach-Zehnder atom interferometer, similar to the one described in [12], is formed using zeroth and first order diffraction from three 100 nm period silicon

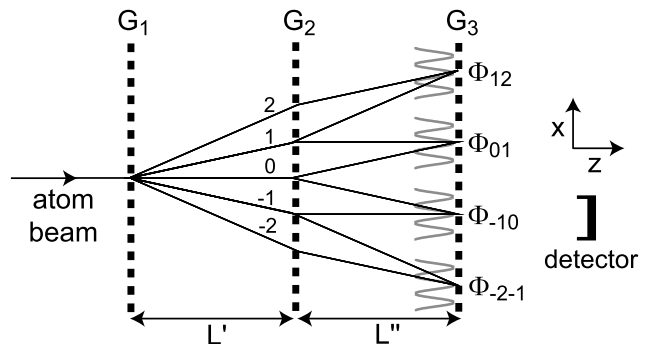


FIG. 1: Diagram of experimental setup for measuring diffraction phases with an atom interferometer. Since the interference pattern is read out using G_3 as a mask, only the paths indicated by the solid lines will lead to a significant interference signal. The mismatch of the grating spacings $\Delta L \equiv L'' - L'$ and the diffraction phases Φ_n induced by G_1 determine the measured interference phases Φ_{mn} .

nitride gratings [13] which are denoted G_1, G_2, G_3 . These gratings are nominally separated by 1 m. A collimated supersonic Na atom beam is first diffracted by grating G_1 , inducing a phase shift which depends on the diffraction order and will be described later. Each diffracted beam then undergoes first order diffraction by G_2 and forms a spatial interference pattern just before G_3 . The atoms transmitted through G_3 are ionized by a $60 \mu\text{m}$ wide hot Re wire and counted by a channel electron multiplier. Grating G_3 is then scanned in the direction transverse to the incident atom beam (x -axis) to determine the phase of the interference pattern. While there are many paths which can interfere at the plane of G_3 only the ones which involve first order diffraction by G_2 (as indicated in Fig. 1) will lead to a significant interference signal because of velocity dispersion and the use of G_3 as a transmission mask. Since each relevant path through G_2 undergoes first order diffraction both paths acquire the same diffraction phase, which means there is no net phase shift induced by G_2 . In addition, grating G_3 acts

as a transmission mask so only the diffraction phases induced by G_1 will lead to a relative phase shift between the interfering paths. In principle, the diffraction phases can then be determined by comparing the phase of the various interferometer outputs which can be measured separately by moving the detector along the x-axis.

In practice there are two types of phase shifts that need to be considered when predicting the relative phase of the various interferometer outputs. One originates from the diffraction phase induced by G_1 and the other from a distance mismatch between the gratings G_1, G_2, G_3 , which is denoted by $\Delta L \equiv L'' - L'$ in Fig. 1. In order to report a measurement of the diffraction phases, expressions for both of these phase shifts will be put forth.

From previous work it has been shown that atomic diffraction from a material grating will create diffracted beams with complex amplitudes ψ_n given by

$$\psi_n = A_n e^{i\Phi_n} \propto \int_{-w/2}^{w/2} e^{i\phi(\xi)} e^{i2\pi\xi n/d} d\xi, \quad (1)$$

where A_n is the amplitude and Φ_n is the diffraction phase for a given diffraction order n as derived in [5, 10, 11]. The variable ξ is the position measured from the center of the grating window whose size is w and grating period is d . The expression in Eqn. 1 is valid in the far-field (Fraunhofer) diffraction regime and is appropriate for our experimental setup as described in [5]. The phase $\phi(\xi)$ represents the phase accumulated by the atom wave as it propagates through the grating window, given by the WKB approximation to leading order in $V(\xi)$ as

$$\phi(\xi) = -\frac{lV(\xi)}{\hbar v}, \quad (2)$$

where l is the thickness of the grating, \hbar is Planck's constant and v is the atom beam velocity [5]. The atom-surface interaction potential $V(\xi)$ in Eqn. 2 is given by

$$V(\xi) = -C_3 \left[\left| \xi - \frac{w}{2} \right|^{-3} + \left| \xi + \frac{w}{2} \right|^{-3} \right], \quad (3)$$

where C_3 is coefficient describing the strength of the vdW interaction. This form of the vdW potential is valid for atom-surface distances of $\lesssim 1\mu\text{m}$ for Na atoms and neglects the finite thickness of the grating bars [5, 8]. A plot of diffraction phases and amplitudes are shown in Fig. 2 as a function of C_3 .

There is also a phase shift between the interferometer outputs induced by a distance mismatch of the gratings G_1, G_2, G_3 along the z-axis. The origin of this phase shift can be understood by recalling that when two plane waves interfere at an angle $\theta = \lambda_{dB} d^{-1}$, interference fringes will be formed with intensity maxima along lines with an angle $\theta/2$ as described in [14]. In other words, a spatial interference pattern of the form $\cos[k_g(x - z\theta/2)]$ with wave number $k_g = 2\pi/d$ will be observed. If the $n = 0, 1$ paths depicted in Fig. 1 are regarded as plane

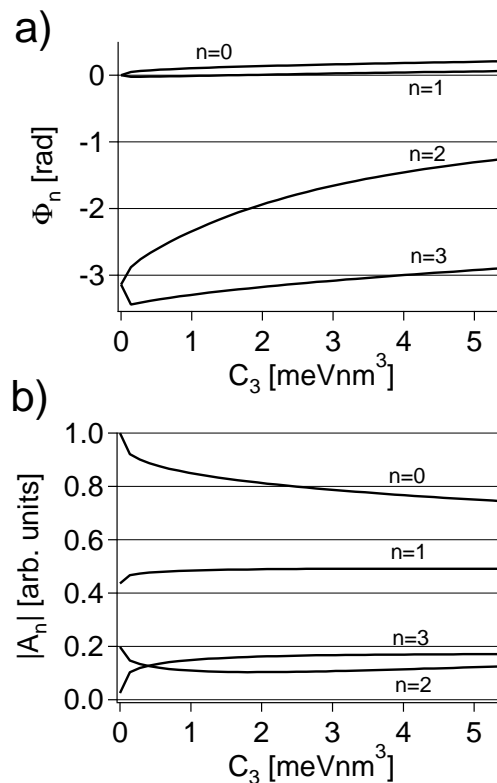


FIG. 2: Plots of the diffraction phases Φ_n and amplitudes A_n as a function of the vdW coefficient C_3 for diffraction orders $n = 0, 1, 2, 3$ according to Eqn. 1. The grating parameters $w = 65$ nm, $l = 150$ nm, $d = 100$ nm, and atom beam velocity $v = 2900$ m/s were used to generate the curves.

waves interfering at an angle $\theta = \lambda_{dB} d^{-1}$ then by geometry an effective phase shift

$$\Phi_{\Delta L} = \frac{\pi \Delta L \lambda_{dB}}{d^2}, \quad (4)$$

will be observed if there is a distance mismatch $\Delta L \equiv L'' - L'$ between the interferometer gratings. For two general paths originating from the diffraction orders m, n of G_1 the effective phase shift induced by ΔL will be given by $(m+n)\Phi_{\Delta L}$, since the fringe maxima are just rotated by an angle $(m+n)\theta/2$ with respect to the z-axis.

The expressions for the diffraction phase Φ_n (Eqn. 1) and grating distance mismatch phase $\Phi_{\Delta L}$ (Eqn. 4) can then be used to specify the wave function $|\chi_{mn}\rangle$ just before grating G_3

$$|\chi_{mn}\rangle = e^{ik_g x} |\psi_m\rangle + e^{i(m+n)\Phi_{\Delta L}} |\psi_n\rangle, \quad (5)$$

for any two interfering paths involving the diffraction orders m, n of grating G_1 . The wave functions $|\psi_m\rangle$ and $|\psi_n\rangle$ describe the two atom beams corresponding to a given interferometer output and accounts for the diffraction phases and amplitudes through the relations

$$\langle \psi_n | \psi_n \rangle \equiv |A_n|^2, \quad (6)$$

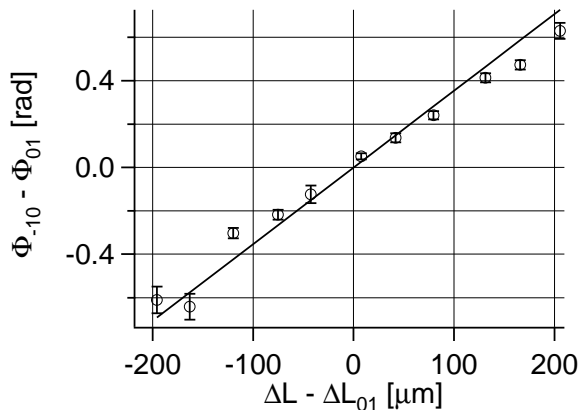


FIG. 3: Measured phase difference as a function of ΔL . The variable ΔL_{01} is the grating distance mismatch required to make the observed phase difference zero. The solid curve contains no free parameters and is the phase difference implied by Eqns. 4 and 9 for the independently measured velocity $v = 2900$ m/s ($\lambda_{dB} = 0.056$ Å) and $d = 100$ nm.

and

$$\langle \psi_n | \psi_m \rangle \equiv A_n^* A_m e^{i(\Phi_m - \Phi_n)}, \quad (7)$$

where A_m, A_n and Φ_m, Φ_n are given by Eqn. 1. The intensity can then be found in the usual way

$$I_{mn}(x) \equiv \langle \chi_{mn} | \chi_{mn} \rangle \propto 1 + C_{mn} \cos(k_g x + \Phi_{mn}), \quad (8)$$

where C_{mn} and Φ_{mn} are the observed contrast and phase for a given interferometer output involving the diffraction orders m, n as depicted in Fig. 1. The measured interferometer phase

$$\Phi_{mn} \equiv (\Phi_m - \Phi_n) - (m + n)\Phi_{\Delta L}, \quad (9)$$

can also be expressed in terms of the diffraction phases Φ_n and grating mismatch phase shift $\Phi_{\Delta L}$. From Eqn. 9 it can be seen that $\Phi_{mn} = -\Phi_{-m-n}$, as implied by the symmetry of the interferometer.

Equations 8 and 9 can now be used to predict the phase shift between the various interferometer outputs shown in Fig. 1. One noteworthy aspect of Eqn. 9 is the possibility for Φ_{mn} to be made zero if the diffraction phase term is cancelled by the appropriate choice of ΔL . To verify this prediction the phase difference $\Phi_{-10} - \Phi_{01} = -2\Phi_{01}$ was measured as a function of ΔL and the results are shown in Fig. 3. The atom beam velocity $v = 2900$ m/s ($\lambda_{dB} = 0.056$ Å) was measured independently by observing the diffraction pattern generated by G_1 when the other gratings are removed. Equations 4 and 9 can then be used to generate the solid curve in Fig. 3, since the grating period is known to be $d = 100$ nm. The data agree quite well with our theory considering that there

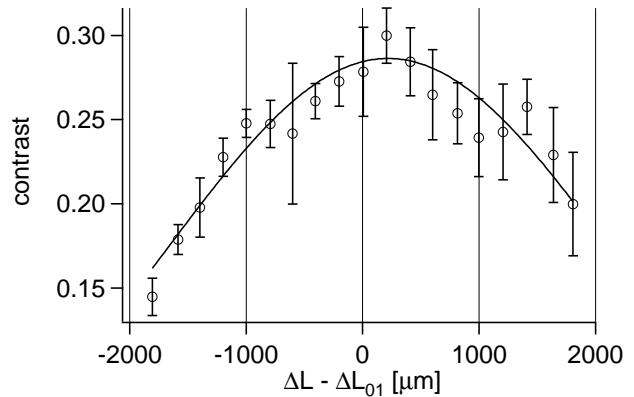


FIG. 4: Measured contrast as a function of the grating distance mismatch ΔL . The solid line is a best fit using Eqn. 10, which led to the determination of $\Delta L_{01} = 218 \pm 72$ μm .

are no free parameters in the solid curve. At this point ΔL is known only up to some offset ΔL_{01} which can be interpreted as the grating distance mismatch which leads to the special case of $\Phi_{\Delta L} = \Phi_0 - \Phi_1$. However, the value of ΔL_{01} will be determined next using another independent measurement technique.

As ΔL is shifted further from zero the partial spatial and temporal coherence of the atom beam causes the measured interference contrast to decrease. This notion is evident in the experimental data presented in Fig. 4, which plots the observed interference contrast as a function of ΔL . This contrast peak can be used to determine the offset ΔL_{01} , which then specifies the value of $\Phi_0 - \Phi_1$ through Eqns. 4 and 9. For our particular atom beam setup spatial coherence was the dominant mechanism responsible for the contrast reduction.

The spatial coherence of the atom beam is determined by the spatial extent of the atom beam source, and describes the correlation of different transverse points of the wave function. When $\Delta L = 1$ mm there is about 60 nm of shear (i.e. transverse displacement) between the two interfering beams, since $\theta = \lambda_{dB} d^{-1} \approx 60$ μrad . As a result the contrast will be reduced because the regions of overlap for the two interfering wave functions will be less correlated when there is nonzero shear. The van Cittert-Zernike theorem states that the contrast will be reduced in a way that is related to the spatial Fourier transform of the atom beam source profile [6]. If the source intensity distribution is assumed to be $w_c^{-1} \text{rect}(xw_c^{-1})$ then the contrast will be reduced according to

$$C = C_o \left| \text{sinc} \left(\frac{w_c s}{\lambda_{dB} z_c} \right) \right| = C_o \left| \text{sinc} \left(\frac{w_c \Delta L}{dz_c} \right) \right|, \quad (10)$$

where w_c is collimation slit width, z_c is distance from the collimation slit to G_3 , and $s = \Delta L \theta$ is the amount of induced shear. Equation 10 is similar to one found in [15] derived using a different method. The best fit

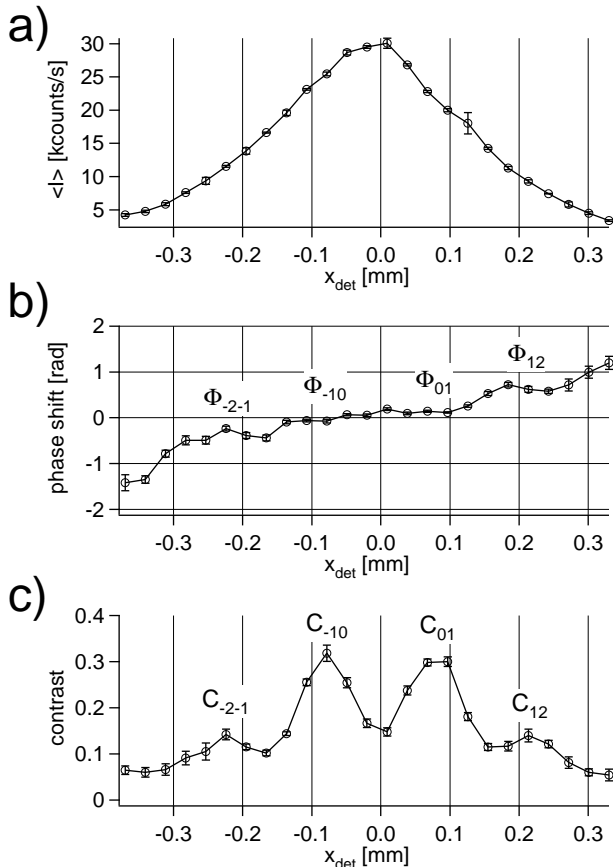


FIG. 5: Measured contrast, phase, and average intensity as a function of detector position. From the contrast profile one can clearly make out the different interferometer outputs as indicated in Fig. 1. The grating distance mismatch ΔL was chosen so that $\Phi_{01} = -\Phi_{-10} \approx 0$.

to the data in Fig. 4 using Eqn. 10 yielded a value of $\Delta L_{01} = 218 \pm 72 \mu\text{m}$. Since $d = 100 \text{ nm}$ and $z_c = 2.8 \text{ m}$, a best fit value of $w_c = 81 \mu\text{m}$ was found to be consistent with the data, according to Eqn. 10.

Given the data in Figs. 3 and 4 the best fit value of ΔL_{01} implies that $\Phi_0 - \Phi_1 = 0.39 \pm 0.13 \text{ rad}$, according to Eqn. 4. The diffraction phase $\Phi_0 = 0.30 \pm 0.15 \text{ rad}$ was measured recently in [11], which yields the first order diffraction phase $\Phi_1 = -0.09 \pm 0.20 \text{ rad}$. This value for Φ_1 is consistent with the value predicted by Eqn. 1, as summarized in Table I.

By moving the detector so that it intercepts the different interferometer outputs indicated in Fig. 1 the higher order diffraction phases can be determined. The measured contrast, phase, and intensity is shown in Fig. 5 as a function of detector position. From Fig. 5 the phase $\Phi_{12} = 0.4 \pm 0.2 \text{ rad}$ can be determined. Equation 9 then implies that $\Phi_1 - \Phi_2 = 1.57 \text{ rad}$, which finally leads to $\Phi_2 = -1.66 \pm 0.48 \text{ rad}$. This value compares well to that predicted by Eqn. 1, as shown in Table I.

In conclusion the atomic diffraction phases Φ_n in-

TABLE I: Measured and calculated values of Φ_n

n	Measured Φ_n [rad]	Predicted ^b Φ_n [rad]
0	0.30 ± 0.15^a	0.16
1	-0.09 ± 0.20	0.02
2	-1.66 ± 0.48	-1.71

^aThis value was measured in [11].

^bValues are calculated with Eqn. 1 and $C_3 = 2.7 \text{ meV nm}^3$ for Na atoms and a silicon nitride surface [5].

duced by a material grating structure have been measured for $n = 0, 1, 2$. This was accomplished by comparing the relative phases of the various outputs of a three-grating Mach-Zehnder atom interferometer. These measurements agree with a simple model that includes a vdW atom-surface interaction between the Na atom beam and the silicon nitride grating. In the future, one could simultaneously monitor Φ_{01} and Φ_{-10} with two detectors, while applying some interaction to say the $n = 1$ arm. One could then perform self-referencing phase measurements with the interferometer, eliminating the need to take control data in a serial fashion. In this type of application knowledge of the diffraction phases observed here would be required.

This work was supported by Research Corporation and the National Science Foundation Grant No. 0354947.

- [1] P. R. Berman, ed., *Atom Interferometry* (Academic Press, 1997).
- [2] M. Weitz, B. C. Young, and S. Chu, *Phys. Rev. A* **50**, 2438 (1994).
- [3] S. Durr, T. Nonn, and G. Rempe, *Nature* **395**, 33 (1998).
- [4] M. Buchner, R. Delhuelle, A. Miffre, C. Robilliard, and J. Vigue, *Phys. Rev. A* **68**, 013607 (2003).
- [5] J. D. Perreault, A. D. Cronin, and T. A. Savas, *Phys. Rev. A* **71**, 053612 (2005).
- [6] M. Born and E. Wolf, *Principles of Optics* (Cambridge University Press, 1999).
- [7] T. L. Gustavson, A. Landragin, and M. A. Kasevich, *Class. Quantum Grav.* **17**, 2385 (2000).
- [8] P. W. Milonni, *The Quantum Vacuum* (Academic Press, 1994).
- [9] R. E. Grisenti, W. Schollkopf, J. P. Toennies, G. C. Hegerfeldt, and T. Kohler, *Phys. Rev. Lett.* **83**, 1755 (1999).
- [10] A. D. Cronin and J. D. Perreault, *Phys. Rev. A* **70**, 043607 (2004).
- [11] J. D. Perreault and A. D. Cronin, arXiv:physics/0505160 (2005).
- [12] D. W. Keith, C. R. Ekstrom, Q. A. Turchette, and D. E. Pritchard, *Phys. Rev. Lett.* **66**, 2693 (1991).
- [13] T. A. Savas, M. L. Schattenburg, J. M. Carter, and H. I. Smith, *J. Vac. Sci. Tech. B* **14**, 4167 (1996).
- [14] E. Hecht, *Optics* (Addison Wesley Longman, 1998).
- [15] C. Champenois, M. Buchner, and J. Vigue, *Eur. Phys. J. D* **5**, 363 (1999).